ELSEVIER

Journal of the Neurological Sciences 189 (2001) 71–81

Journal of the Neurological Sciences

www.elsevier.com/locate/jns

Opsoclonus in three dimensions: oculographic, neuropathologic and modelling correlates

Agnes M.F. Wong [a,b], Sam Musallam [c], R.D. Tomlinson [c], Patrick Shannon [d], James A. Sharpe [a,b,*]

[a] *Division of Neurology, University Health Network, Toronto Western Hospital, Toronto, Ontario, Canada*
[b] *Department of Ophthalmology, University Health Network, Toronto Western Hospital, Toronto, Ontario, Canada*
[c] *Department of Physiology, University of Toronto, Toronto, Ontario, Canada*
[d] *Division of Neuropathology, University Health Network, Toronto Western Hospital, Toronto, Ontario, Canada*

Received 30 January 2001; received in revised form 18 May 2001; accepted 26 June 2001

Abstract

Opsoclonus is a dyskinesia consisting of involuntary, arrhythmic, chaotic, multidirectional saccades, without intersaccadic intervals. We used a magnetic scleral search coil technique to study opsoclonus in two patients with paraneoplastic complications of lung carcinoma. Eye movement recordings provided evidence that opsoclonus is a three-dimensional oscillation, consisting of torsional, horizontal, and vertical components. Torsional nystagmus was also present in one patient. Antineuronal antibody study revealed the presence of anti-Ta (Ma2 onco-neuronal antigen) antibodies in one patient, which had previously been associated only with paraneoplastic limbic encephalitis and brainstem dysfunction, but *not* opsoclonus, and only in patients with testicular or breast cancer. Neuropathologic examination revealed mild paraneoplastic encephalitis. Normal neurons identified in the nucleus raphe interpositus (rip) do not support postulated dysfunction of omnipause cells in the pathogenesis of opsoclonus. Computer simulation of a model of the saccadic system indicated that disinhibition of the oculomotor region of the fastigial nucleus (FOR) in the cerebellum can generate opsoclonus. Histopathological examination revealed inflammation and gliosis in the fastigial nucleus. This morphological finding is consistent with, but not necessary to confirm, damage to afferent projections to the FOR, as determined by the model. Malfunction of Purkinje cells in the dorsal vermis, which inhibit the FOR, may cause opsoclonus by disinhibiting it.

Keywords: Opsoclonus; Paraneoplastic syndrome; Fastigial nucleus; Fastigial oculomotor region; Search coils; Oculography; Computer simulation; Neuropathology

1. Introduction

Opsoclonus is a dyskinesia consisting of involuntary, arrhythmic, chaotic, multidirectional saccades, without intersaccadic intervals [1–5]. In adults, the most common causes of opsoclonus include parainfectious brainstem encephalitis, paraneoplastic, and metabolic–toxic states [1,6]. In many cases, the cause is never established [1]. Such saccadic oscillations differ from nystagmus in that the phase that takes the eye off the target is always a saccade, not a smooth eye movement. In contrast to ocular flutter, which consists of horizontal back-to-back saccades, opsoclonus is multidirectional [1,2,7]. The pathogenesis of opsoclonus is uncertain. Damage to omnipause cells in the brainstem [8,9] or to the cerebellum [10–13] has been implicated. We report the oculographic and neuropathologic features of opsoclonus in two patients with paraneoplastic syndrome. Computer simulation of a saccadic system model indicated that damage of afferent projections to the oculomotor region of the fastigial nucleus (FOR) could generate opsoclonus.

2. Patients and methods

2.1. Patient 1

An 81-year-old woman presented with a 6-month history of progressive gait unsteadiness, hoarseness of voice, and blurry vision. She had a 25-lb weight loss over 3 months. Past medical history included chronic atrial fibril-

* Corresponding author. Division of Neurology, University Health Network, EC 5-042, Toronto Western Hospital, 399 Bathurst Street, Toronto, Ontario, Canada M5T 2S8. Tel.: +1-416-603-5950; fax: +1-416-603-5596.

E-mail address: sharpej@uhnres.utoronto.ca (J.A. Sharpe).

0022-510X/01/$ - see front matter
PII: S0022-510X(01)00564-0

lation. Her medications included digoxin, sotalol, warfarin and lorazepam. She smoked cigarettes for 50 years.

On admission, visual acuity was 20/50 in each eye. Pupils, visual fields, and fundi were normal. The range of ductions was full. She had torsional jerk nystagmus, beating clockwise with respect to the patient. In addition, bursts of oblique and torsional rapid eye movements were observed during fixation, smooth pursuit, convergence and eyelid closure. Smooth pursuit movements were saccadic. Saccades were hypermetric. She had a mild dysarthria. Muscle bulk, tone and power were normal. There was no myoclonus. Finger-to-nose and heel-to-shin testing showed severe bilateral ataxia. Tendon reflexes were symmetrical and plantar responses were flexor. Sensory examination was normal. Her gait was ataxic.

Blood tests including white cell count, hemoglobin, erythrocyte sedimentation rate, glucose, urea and creatinine were normal. Serologic tests for syphilis, HIV and HTLV were negative. Magnetic resonance imaging of the head showed only a few patchy areas of signal change consistent with microangiopathic lesions in the brainstem and basal ganglia. CSF study revealed a few lymphoid cells, and normal glucose and protein. Bacterial, viral and fungal cultures of CSF were negative.

Search for malignancy disclosed a left hilar mass and left apical nodule on chest CT with contrast. Biopsy of the hilar mass showed a poorly differentiated non-small cell carcinoma. Antineuronal antibody study was positive for anti-Ta (Ma2 onco-neuronal antigen) antibodies, which are usually associated with testicular cancer [14] or breast cancer [15].

The patient received trials of clonazepam, and then gabapentin therapy without improvement in her eye movements. She deteriorated rapidly and developed a limbic dementia, with memory loss and personality change. She declined further treatment and died from respiratory failure 6 weeks after presentation. Consent for autopsy was obtained.

2.2. Patient 2

A 76-year-old man presented with a 3 week history of oscillopsia, loss of balance, vertigo, fatigue, anorexia and a 15-lb weight loss over 2 months. Past medical history included transient ischemic attack, for which he took aspirin daily. He smoked cigarettes for 60 years.

Visual acuity was 20/70 in each eye. Pupils, visual fields, and fundi were normal. The range of ductions was full. Bursts of oblique and torsional rapid eye movements, which increased during convergence and upgaze, and decreased during fixation, were observed. Saccades were hypermetric. He had severe dysarthria. Muscle bulk, tone and power were normal. There was no myoclonus. Coordination testing revealed bilateral intention tremor, dysmetria and dysdiadochokinesia. Tendon reflexes were symmetrical and plantar responses were flexor. Sensory examination was normal. He had truncal and gait ataxia.

Magnetic resonance imaging of the head showed several old infarcts in both hemispheres and the pons. CSF study revealed a few lymphoid cells, normal glucose and protein. Bacterial, viral and fungal cultures of CSF were negative.

Chest CT with contrast revealed a mass extending from the left upper lobe to the left hilum. Biopsy of the hilar mass showed a mixed large and small cell carcinoma of the lung. Anti-Purkinje cell antibodies were negative. The patient received palliative care and died from respiratory failure 5 months after presentation. Permission for autopsy was not given.

2.3. Oculographic study

2.3.1. Visual stimuli and experimental protocol

Eye position was measured with search coils while patients fixated a red laser spot of 0.25° in diameter, rear-projected onto a vertical flat screen 1 m away from the naision. Spontaneous eye movements were recorded in light while patients viewed the laser target in mid-position, and in total darkness.

To investigate the dynamics of saccades, patients were instructed to follow the laser spot as it stepped among positions, while one eye was occluded. The laser spot started in the center, then stepped to the 10° right position, then back to center, then 10° left, cycling through this pattern 20 times for each eye. At each position, the laser halted for 3 s. Recordings were then made with the other eye fixating and the fellow eye occluded. To avoid fatigue, breaks were provided approximately every 2 min for 1–3 min.

2.3.2. Recordings of eye movement and calibration

Eye positions were measured by a three-dimensional magnetic search coil technique, using a 6 ft (183 cm)

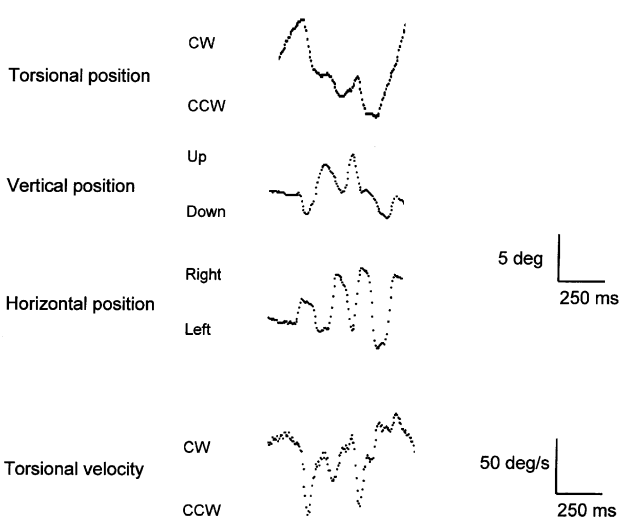

Fig. 1. Magnetic scleral search coil recordings showing opsoclonus in patient 1. The opsoclonus consists of burst of irregular, conjugate, back-to-back saccades with torsional, vertical and horizontal components (only the right eye is shown).

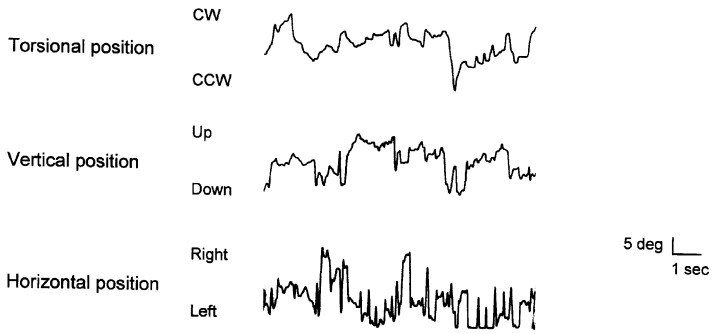

Fig. 2. Magnetic scleral search coil recordings showing the torsional, vertical and horizontal components of opsoclonus in patient 2 (only the right eye is shown).

diameter coil field arranged in a cube (CNC Engineering, Seattle, WA). In each eye, patients wore a dual-lead scleral coil annulus designed to detect horizontal, vertical, and torsional gaze positions (Skalar Instrumentation, Delft, Netherlands). Horizontal and vertical movements were calibrated with the coil mounted on a rotating protractor, and confirmed by testing eye positions during periods of relatively steady fixation of a target $\pm 10^{\circ}$ above, below and beside the mid-position. Torsional movements were calibrated by attaching the scleral coil to a rotating protractor. Torsional precision was about $\pm 0.2^{\circ}$. Large horizontal and vertical movements produced small crosstalk deflections in the torsional channel of less than 4% of the amplitude of the horizontal and vertical movement. Consistency of calibrated positions after each eye movement provided evidence that the coil did not slip on the eye. Eye position data were digitized at 200 Hz. They were recorded on disc for off-line analysis. Analog data were also displayed in real time by a rectilinear ink-jet polygraph (Elema-Schönander, Stockholm).

Eye position signal was digitally differentiated to yield eye velocity using a 10-point moving window technique. For each eye movement with a velocity step greater than $20^{\circ}/\mathrm{s}$, peak velocity was marked. For each selected peak velocity, the time when the eye velocity surpassed or dropped below 5% of maximum velocity was taken as the beginning and the end of a saccade. Cursors then marked the beginning and end of saccades in the corresponding eye position channel.

2.3.3. Data analyses

Asymptotic velocities of horizontal, vertical and torsional saccades were derived by computer analysis of velocity–amplitude scatter plots using an exponential best fit curve:

$$\mathrm{PV} = V(1 - \mathrm{e}^{-A/C})$$

where PV is peak velocity at any point on the curve, V is asymptotic velocity, A is saccade amplitude, and C is a constant.

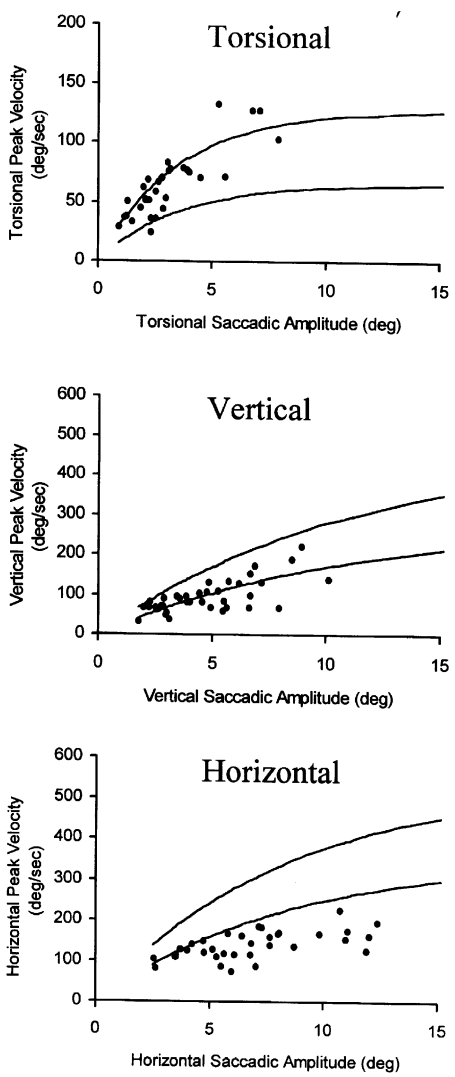

Fig. 3. Plots of peak velocities versus amplitude (main sequence) in paraneoplastic opsoclonus and normal subjects. Solid lines represent one standard deviation above and below the mean peak velocity in normal subjects. Vertical and horizontal peak velocities were obtained during performance of saccade tasks in 26 normal subjects [16,17], whereas torsional peak velocities were obtained from quick phase data during torsional VOR in 10 normal subjects (unpublished data). Scattered dots represent saccades from the oscillations in patient 1.

For horizontal and vertical saccades, we used data from 26 normal subjects [16,17] (16 women; mean age = 61 ± 7 years; median age = 62; age range = 37–84). Because voluntary torsional saccades cannot be elicited [18], torsional saccades data were obtained from 10 normal subjects (5 women; mean age = 49 years; median age = 55; age range = 19–69) by analyzing quick phases during dynamic head roll. While subjects viewed a laser target at 1 m, active vestibular responses were elicited pseudo-sinusoidally in roll at frequencies of about 0.5, 1 and 2 Hz, and amplitudes of about 10°. Quick phases of vestibular nystagmus were identified by a computer program using velocity and acceleration criteria [19]. The velocity and amplitude of torsional quick phases were calculated.

Statistical analyses were performed using Student's *t*-tests, two-tailed, unequal variance. Values were defined as significant when $p < 0.05$.

2.4. Neuropathologic study

The brain, spinal cord, and specimens of dorsal root ganglion, peripheral nerve and skeletal muscle of patient 1 were immersion fixed in formalin, and processed according to routine protocols. The midbrain, pons and upper medulla were serially sectioned at 60-μm intervals and stained with Luxol-Fast Blue and Hematoxylin/Eosin, and Luxol-Fast Blue/Cresyl Violet to identify the appropriate anatomical structures. Where appropriate, immunohistochemical staining for CD3 (1:1000, Dako), CD4 (1:50, Dako), CD8 (1:50 Novocastra), CD57 (1:200, Dako), CD56 (1:100, Zymed), CD57 (1:200 PharMingen), GFAP (1:10000, Dako), CD68 (1:200, Dako), CD20 (1:500, Dako) and CD79a (1:200, Dako) was also performed, as were immunofluorescence studies for C3 (1:20 Dako) and IgG (1:20, Dako).

3. Results

3.1. Oculographic recordings

Multiple intermittent bursts of irregular, conjugate, back-to-back rapid eye movements with torsional, vertical and horizontal components were evident in both patients (Figs. 1 and 2). Peak velocities of these saccadic oscillations in patient 1 were plotted against their amplitude, and compared with the main sequence of normal subjects (Fig. 3). The peak velocities of all three components (torsional, vertical and horizontal) were within two standard deviations of the normal main sequence, confirming their normal saccadic structure.

During fixation, torsional nystagmus with slow phases that rotate the upper poles of the eyes toward the right shoulder (designated clockwise; that is, from the patient's viewpoint) was observed intermittently in patient 1. The slow phase had mixed accelerating, constant and decelerating waveforms, with an average velocity of 33°/s (Fig. 4). The counterclockwise beating nystagmus quick phases had a mean peak velocity of 72°/s, and an average amplitude of 5° (Fig. 4).

Horizontal saccades made during 10° target steps were hypermetric in both patients. Saccadic gain during *abduction* was 11.4 ± 0.8 in patient 1 and 11.2 ± 0.7 in patient 2, compared with 8.4 ± 1.3 in normal controls (*Z*-tests, $p < 0.05$). During *adduction*, saccadic gain was 11.3 ± 1.1

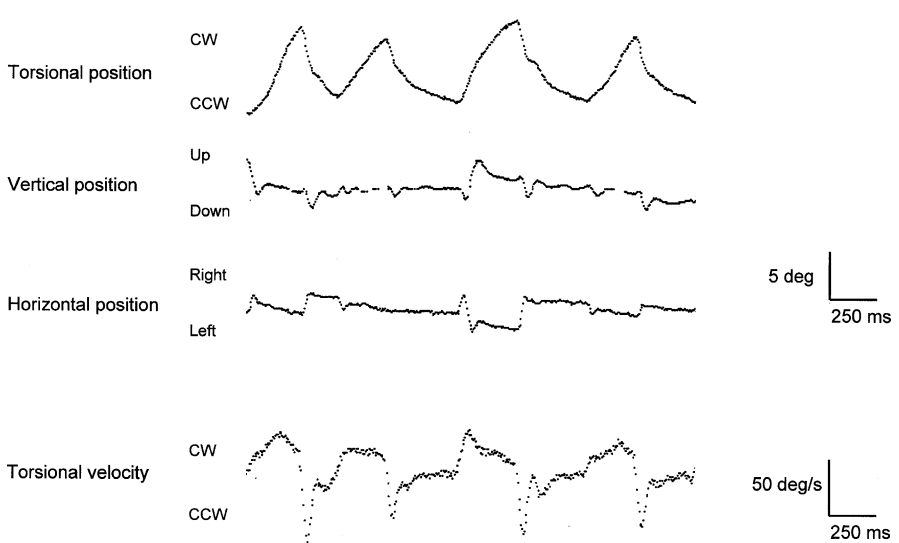

Fig. 4. Magnetic scleral search coil recordings showing conjugate torsional nystagmus (only the right eye is shown) in patient 1. The torsional nystagmus consists of slow phase that rotated the eyes toward the right shoulder (designated clockwise; that is, from the patient's viewpoint), followed by corrective quick phases in the opposite direction.

in patient 1 and 11.2 ± 0.8 in patient 2, compared with 8.3 ± 1.4 in normal controls (Z-tests, $p < 0.05$).

3.2. Neuropathologic findings

At autopsy, a small focus of anaplastic large cell carcinoma was found in the apex of the left lung of patient 1. Isolated metastases to left para-bronchial lymph nodes were identified. No other metastasis was present. No gross or microscopic abnormality was identified in the cerebral cortex. Sections of the brainstem revealed occasional perivascular lymphocytic cuffing, most prominent in the periaqueductal gray matter. The lymphocytic infiltrates were composed of predominantly CD3(+) T cells. Of these, the majority were interstitial and perivascular CD8(+) T cells, with a minority of predominantly perivascular CD4(+) T cells. Where CD8(+) T cells were present, there was a background of CD68(+) microglial cell activation and proliferation. No natural killer cells (CD57 or CD56) were detected. Very occasional perivascular CD20(+) and CD79a(+) B cells were found. Immunofluorescence study revealed no intraparenchymal IgG, or C3.

Inflammatory infiltrates were sparse and found in the periaqueductal gray and, to a lesser extent, the pretectum, the substantia nigra, the medial geniculate body, the pulvinar, the superior colliculus, the inferior colliculus and the interstitial nucleus of Cajal (INC). Mild neuronal loss was most apparent in the periaqueductal gray, although all of the areas affected showed mild gliosis. The medial longitudinal fasciculus (MLF), third, fourth and sixth cranial nerve nuclei, the rostral interstitial nucleus of MLF (riMLF) and the nucleus raphe interpositus (rip) were spared, lacking inflammation, neuronal loss or gliosis (Fig. 5).

Examination of the cerebellum revealed some gliosis in the cerebellar roof nuclei, including the fastigial and dentate nuclei (Fig. 6), accompanied by microglial activation and mild lymphocytic infiltration. The cerebellar cortex, including the flocculus and nodulus, showed mild patchy Purkinje cell loss, not incompatible with the patient's age.

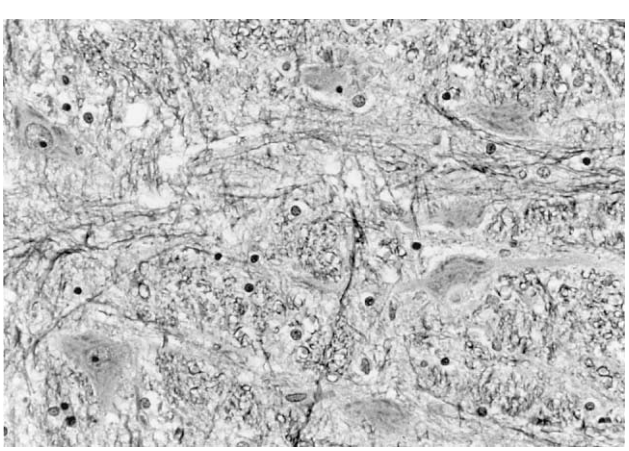

Fig. 5. High-power photomicrograph showing normal nucleus raphe interpositus in patient 1 (hematoxylin–eosin, ×300).

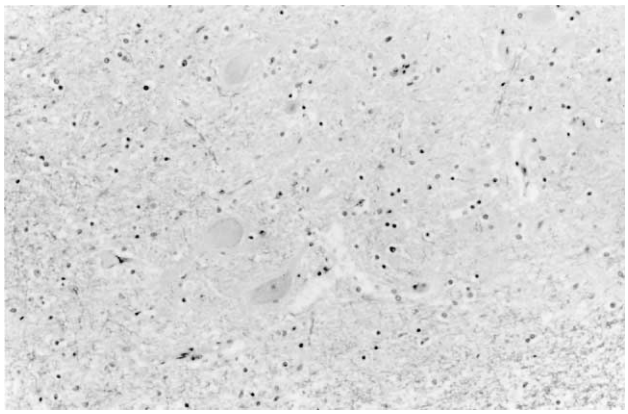

Fig. 6. High-power photomicrograph of the cerebellar roof nuclei, including fastigial nucleus, showing subtle microglial activation in patient 1 (hematoxylin–eosin, ×300).

4. Discussion

4.1. Oculographic characteristics of opsoclonus

Opsoclonus is a dyskinesia consisting of involuntary, irregular, multidirectional saccades, without intervals between sequential saccades [1,2,4,8]. There have been few reports with oculographic documentation [20–22]. Those reports [20–22] were limited by the use of electro-oculography that does not detect torsional movement or adequately resolve vertical motion. Our recordings provide evidence that torsional saccades are a feature of opsoclonus; it is a three-dimensional oscillation.

4.2. Torsional nystagmus and paraneoplastic syndrome

Torsional nystagmus is associated with brainstem lesions that disrupt the central vestibular pathway [23–26]. Non-rhythmic, conjugate torsional eye movement has been observed as a possible paraneoplastic phenomenon [27], but the nature of the movement was not described. Our recordings demonstrated that torsional jerk nystagmus can be associated with paraneoplastic syndrome. The nystagmus of patient 1 consisted of slow phases that rotate the upper poles of the eyes toward the patient's right shoulder (clockwise), each followed by counterclockwise quick phases. The slow phases exhibited mixed accelerating, constant and decelerating waveforms. This contrast with opsoclonus in which the oscillations are initiated by fast eye movements [5]. Central imbalance of inputs from the anterior and posterior semicircular canals on the right side can explain the counterclockwise torsional nystagmus in patient 1 [23].

4.3. Autoantibodies and paraneoplastic opsoclonus

Several autoantibodies that react with both the nervous system and the causal cancer have been detected in patients with paraneoplastic opsoclonus. They include anti-Ri [14,28], anti-Hu [29], and anti-neurofilament protein antibodies [30]. Our patient (patient 1) with non-small cell carcinoma of the lung and paraneoplastic opsoclonus was found to have anti-Ta (Ma2 onco-neuronal antigen) antibodies, which have been associated only with paraneoplastic limbic encephalitis and brainstem dysfunction, but *not* opsoclonus. The presence of anti-Ta antibodies had not been previously identified in any patient with paraneoplastic complications apart from testicular [14] and breast cancer [15].

4.4. Pathogenesis of opsoclonus

4.4.1. Role of omnipause neurons

The pathogenesis of opsoclonus is uncertain. Involvement of various sites in the brainstem and cerebellum have been postulated. In some reports, because of lack of eye movement recordings, it is uncertain as to whether the patients had opsoclonus rather than macrosaccadic oscillations. One hypothesis [8], using a non-ballistic model of the saccadic system, proposed that opsoclonus might result from damage to omnipause cells that are found in the nucleus raphe interpositus (rip) adjacent to the midline of the paramedian pontine reticular formation (PPRF). Omnipause cells inhibit saccade burst neurons in the PPRF and riMLF, preventing unwanted saccades. According to that hypothesis [8], saccadic oscillations occur when the pause cells fail to tonically inhibit the burst neurons; this could occur if (1) an inappropriate and prolonged saccadic trigger signal inhibits the pause cells; (2) the bias signal, which normally tonically excites the pause cells between saccades, is not adequate to maintain the omnipause cell tonic discharge rate; or (3) the omnipause cells themselves cannot respond to the bias signal [8]. However, experimental lesions of omnipause neurons cause slowing of saccades, not saccadic oscillations [31]. Furthermore, although a complete absence of omnipause cells was reported in one patient with paraneoplastic opsoclonus [9], we and others [32] demonstrated absence of any histopathologic change in omnipause cells in our four patients. Particular attention was given to the nucleus raphe interpositus (rip) where the omnipause neurons reside. Omnipause cells of normal appearance were found. The lack of microscopic evidence of abnormality in omnipause cells suggests that opsoclonus is caused by omnipause cells dysfunction that is not evident at microscopic resolution, or that damage to omnipause cells is neither necessary nor sufficient to cause opsoclonus.

4.4.2. Role of the cerebellum

Cerebellar dysfunction has also been invoked in the pathogenesis of opsoclonus in view of damage to Purkinje cells, granular cells and the dentate nuclei in patients with opsoclonus [10–13]. However, these cerebellar changes also occur in patients with paraneoplastic cerebellar degeneration who do *not* have opsoclonus. Moreover, partial ablations of the cerebellar cortex [33] or cerebellectomy including the deep nuclei [33,34] have not been observed to cause opsoclonus in monkeys. Inactivation of the caudal fastigial nucleus of the cerebellum produces saccadic overshoot dysmetria with intervals between sequential saccades, not opsoclonus [35,36]. In our patient, the cerebellar cortex showed decrease in Purkinje and granular cells, but that might be consistent with the patient's age. There was mild gliosis and inflammation in the emboliform, fastigial and dentate nuclei.

4.4.3. The fastigial oculomotor region (FOR)

The caudal part of the fastigial nucleus, the fastigial oculomotor region (FOR), is important for the control of saccade accuracy and consistency [33,37,38]. In addition to receiving inhibitory inputs from Purkinje cells of the dorsal vermis of lobules VIc and VII, the FOR receives projections from the frontal eye fields and superior colliculus, via the nucleus reticularis tegmenti pontis (NRTP) [39]. Projections of the fastigial nucleus decussate within the cerebellum and enter the uncinate fasciculus, which courses along the dorsolateral border of the brachium conjunctivum, to reach the brainstem. Within the brainstem, FOR projections terminate onto omnipause neurons, burst neurons, and the rostral pole of the superior colliculus [39,40]. Because the burst neurons in the paramedian pontine reticular formation (PPRF) and the rostral interstitial nucleus of the medial longitudinal fasciculus (riMLF) generate horizontal, vertical and torsional saccades, FOR projections to these burst neurons make it a suitable candidate in the pathogenesis of abnormal saccadic oscillations in all three dimensions. We propose a saccadic system model that incorporates the FOR, in a feedback loop, into the brainstem saccade-generating mechanism.

Neurons in the FOR fire during both ipsilateral and contralateral saccades [41–44]. The contralateral FOR neurons burst before the onset of saccade, and their firing onset is not correlated with any property of the saccade [41]. Conversely, the time of onset for neurons in the ipsilateral FOR varies, with bursts occurring later for larger saccades [41]. Thus, as saccade amplitude increases, the difference in time of onset between contralateral and ipsilateral FOR activity increases. Indeed, given any two bursts that are separated, but overlapping, in time (Fig. 7A), their difference can be viewed as an acceleration followed by a deceleration (Fig. 7B). By taking the double integral of their difference, a plot of the change in position over time can be obtained, with a profile similar to that of a saccade (Fig. 7C). In addition, when the second burst occurs later in time, as in Fig. 7D (compare with Fig. 7A), the final position reached and hence the amplitude of the saccade increases (compare Fig. 7F with Fig. 7C). This

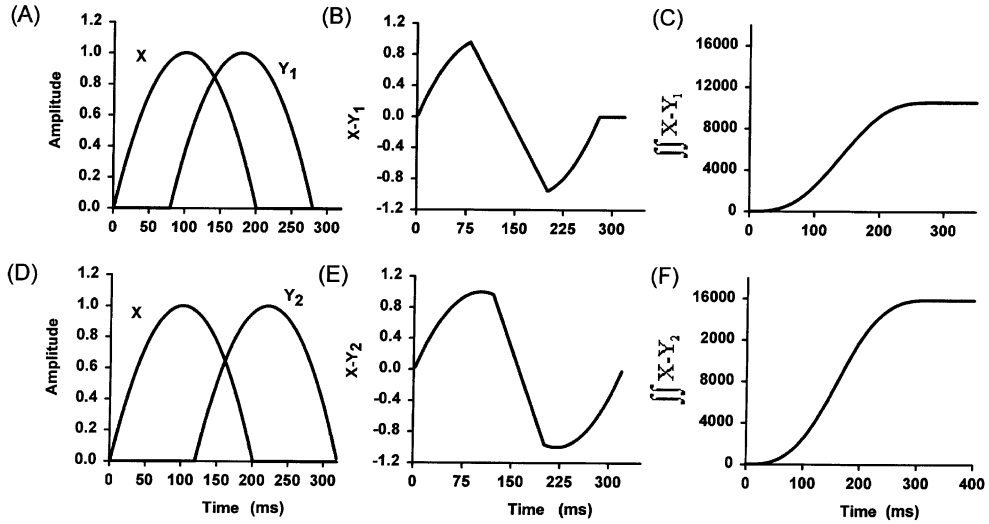

Fig. 7. Computer simulation. Given any two bursts that are separated, but overlapping, in time (A), their difference can be viewed as an acceleration followed by a deceleration (B). By taking the double integral of their difference, a plot of the change in position over time can be obtained, with a profile similar to that of a saccade (C). In addition, when the second burst occurs later in time, as in (D) (compared with A), the final position reached and hence the amplitude of the saccade increases (F) (compared with C).

property has also been observed in the time of onset of ipsilateral FOR activity, and explains why the firing rates of neurons in the FOR correlate with the acceleration of the eye during a saccade.

4.4.4. Model of opsoclonus

Our model for the pathogenesis of opsoclonus was constructed in three steps: (1) selection of an appropriate brainstem saccadic system model [45,46]; (2) incorporation of a feedback loop into the brainstem model such that output from the ipsilateral and contralateral FOR is fed into the brainstem saccadic circuitry, and adjustment of the gain in the brainstem model so that main sequence saccades are generated with the addition of the FOR; and (3) computer simulations to generate abnormal saccades and saccadic oscillations when the FOR is disinhibited.

Several models of saccade generation have been proposed [37,38,45–47]. Given available information about brainstem–cerebellar interaction, we selected the Van Gisbergen et al. [46] model; it employs few assumptions regarding cerebellar contributions to non-adaptive properties of saccades and generates accurate saccades. Fig. 8A shows a simplified schematic diagram of the model [45]. Briefly, a motor error signal is generated by the comparator (labeled as 'C' in Fig. 8A), which continuously compares the desired eye position with an estimate of the current eye position. The resultant motor error signal is used to drive the excitatory burst neurons, which generate the saccadic pulses. An efference copy of the burst neuron discharge is sent to the neural integrator, where the velocity command from the burst neurons is integrated to provide an estimate of current eye position, thus forming an internal feedback loop. Evidence supporting this model has been extensively reviewed [48].

Next, we placed FOR in a feedback pathway and fed its output into the comparator of the brainstem saccadic system, as has been suggested previously [49]. Fig. 8B shows a schematic diagram of our model; the detailed connections are shown in Appendix A. Although controversies exist [38,47,50–54], it is generally believed that the superior colliculus is not part of the local feedback loop [38,47,50,51]. We, therefore, did not include the superior colliculus in our model.

The FOR was modeled as two bursts that are separated in time. Specifically, the first burst, arising from the contralateral FOR, is the result of a saccade plan, arising from input from the lateral intraparietal area, frontal eye fields or superior colliculus (Fig. 8B) [39]. This initial burst was modeled as being proportional to the approximate velocity profile that the burst neurons must output in order to produce an accurate saccade. The second burst, arising from the ipsilateral FOR (Fig. 8B), determines the amplitude of the saccade. We modeled the second burst by passing the output of the brainstem saccadic circuitry through a high pass filter with a time constant of 9 ms (a pole at 111.11, effectively obtaining eye velocity). Saccades of different amplitudes are produced by adjusting the delay in time of onset of activity between the contralateral and ipsilateral FOR. The delays used in our model were 0 ms for a 5° saccade, 2 ms for a 10° saccade, 4 ms for a 15° saccade, 7 ms for a 20° saccade, and 12 ms for a 30° saccade. These values are consistent with experimental values obtained from macaque monkeys [41] and those used for a model of FOR [49].

4.4.5. Computer simulations

To test our model, we adjusted the brainstem saccadic circuitry to assess whether main sequence saccades could

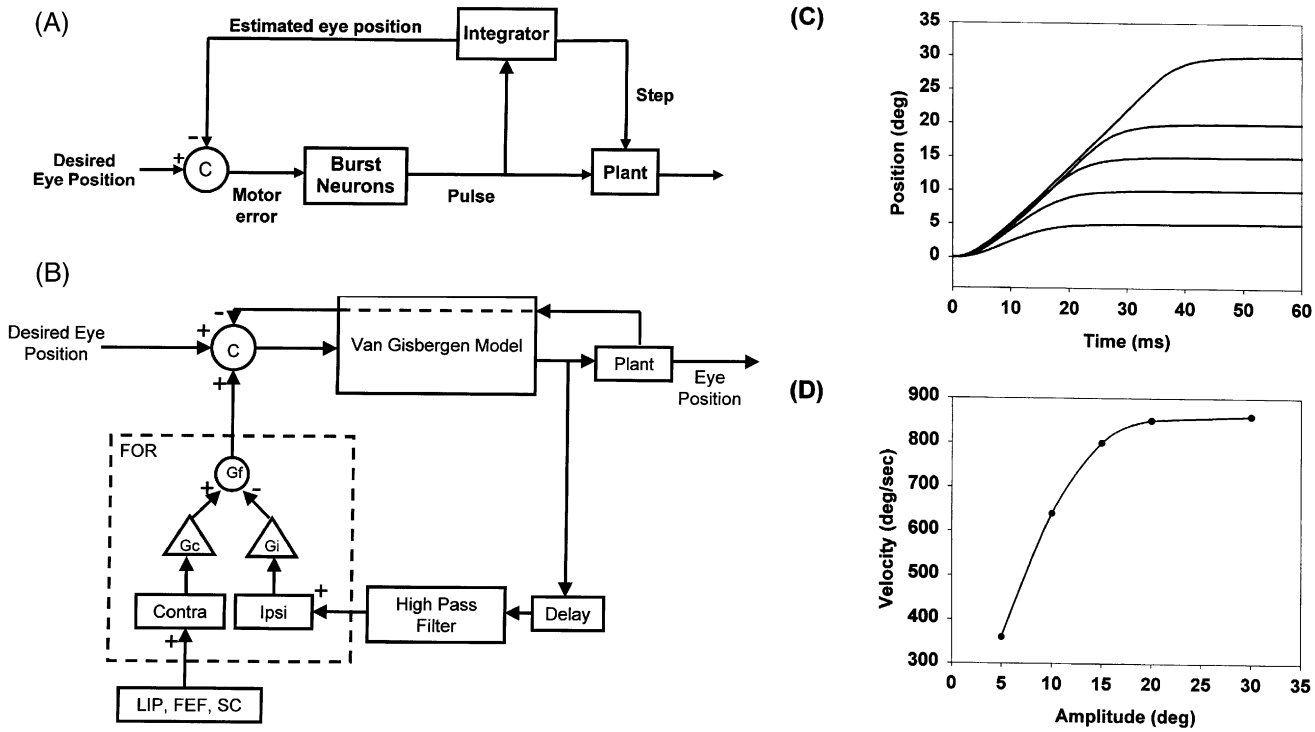

Fig. 8. (A) A simplified schematic diagram of the feedback model proposed by Robinson [45], and used by Van Gisbergen et al. [46], to model the brainstem saccade-generating mechanism. C is the comparator. (B) Proposed model of opsoclonus. The ipsilateral FOR is placed in a feedback loop, and the output of the "cerebellum" is fed into the comparator of the Van Gisbergen et al. [46] model. To produce hypermetric saccades, the internal feedback gain in the Van Gisbergen et al. [46] model is reduced. By adjusting the gain of the FOR, normal saccades (C) with velocity that fall on the main sequence (D) are generated. LIP, lateral intraparietal area; FEF, frontal eye field; SC, superior colliculus; Ipsi, ipsilateral FOR; Contra, contralateral FOR; Plant, orbital tissue.

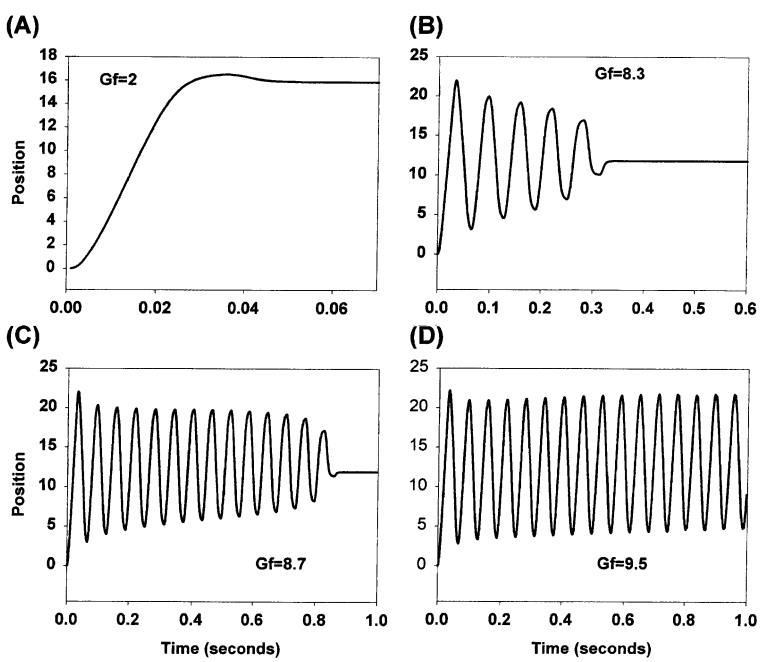

Fig. 9. Computer simulation of our model for saccadic oscillations. Disinhibition of the FOR was achieved by increasing the delay of the feedback loop ('delay' in Fig. 8B and Appendix A) to ipsilateral FOR to 20 ms, and by increasing the gain of the feedback pathway (Gf in Fig. 8B and Appendix A). (A) Increasing the gain of the feedback loop (gain = 2.0) results in a small saccade hypermetria. Further increase in the gain results in oscillations with a time constant proportional to the gains (B; gain = 8.3) and (C; gain = 8.5). The frequency (15 Hz) and amplitude (20°) of the oscillations are consistent with those observed in opsoclonus. As the gain increases further, the system oscillates indefinitely (D; gain = 9.5).

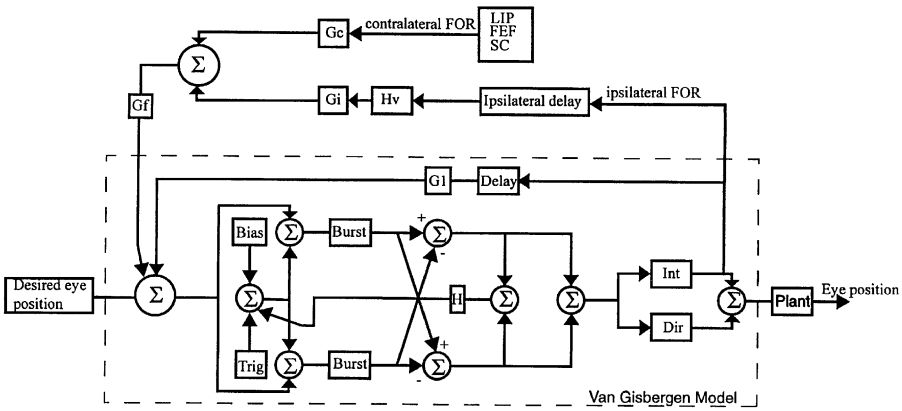

Fig. 10. Model of opsoclonus. Gf is the feedback gain; Gc is the contralateral FOR gain; Gi is the ipsilateral FOR gain; H_v is the high pass filter; ipsilateral delay is the delayed used to induce oscillations in the system. G1 is the adjustment we introduced in the brainstem saccadic circuitry so that incorporation of FOR produces main sequence saccades. The parts of the model that are within the dashed box are from the original Van Gisbergen et al. [46] model. G1 is 0.72, as compared to 1.0 in the original model [46]. Trig is trigger; *H* is gain; Int is integrator; Dir is direct pathway. See text in Appendix A for explanation.

be generated with the incorporation of FOR. Specifically, we reduced the feedback weight (the output of the integrator into the comparator in Fig. 8A) in the brainstem saccade-generating circuitry to produce hypermetric saccades. We then adjusted the weight of the output of FOR to remove the dysmetria (Fig. 8B). Fig. 8C and D show that the model produces accurate saccades and velocity curve that are consistent with previous experimental data [41,49]. We also tested our model by unilaterally inactivating the FOR. In agreement with experimental data from monkeys [35], eliminating one FOR leads to hypermetric ipsiversive saccades and hypometric contraversive saccades.

We then investigated whether *disinhibition*, in contrast to *inactivation*, of the fastigial nucleus could produce saccadic oscillations. We modeled disinhibition of the FOR by increasing the delay in the time of onset of the ipsilateral (second) burst, and by increasing the gain of the feedback pathway (the output of FOR). Fig. 9 depicts the oscillations achieved by the model when a delay of 30 ms was introduced into the ipsilateral (second) burst, while the gain of the feedback pathway increased. A slight increase in the gain of the feedback loop leads to a slight hypermetria (Fig. 9A), just as we recorded in both of our patients with opsoclonus. Further increase in the gain of the feedback loop resulted in oscillations with a time constant proportional to the gain (Fig. 9B and C). The frequency (15 Hz) and amplitude (20°) of the oscillations are consistent to those observed in opsoclonus. As the gain increases further, the system oscillates indefinitely (Fig. 9D). Indeed, the amplitude, frequency and decay of the oscillations can be varied by adjusting the feedback gain and the imposed feedback delay. This model demonstrates that disinhibition of the FOR can account for opsoclonus and the saccade hypermetria that accompanies it.

In closing, we present oculographic evidence of the three-dimensional structure of paraneoplastic opsoclonus, and demonstrate that torsional nystagmus can be associated with paraneoplastic syndrome. Patient 1 was also novel for anti-Ta antibodies being detected in paraneoplastic opsoclonus. The lack of microscopic evidence of abnormality in omnipause cells in our patient and others [32], and the absence of opsoclonus after chemical ablation of omnipause cells [31], suggests that opsoclonus is caused by omnipause cell dysfunction that is not evident at microscopic resolution, or that damage to omnipause cells is neither necessary nor sufficient to cause opsoclonus. Computer simulation of a model of the saccadic system indicated that disinhibition, not inactivation, of the FOR can generate opsoclonus. Histopathological examination revealed inflammation and gliosis in the fastigial nucleus. This morphological finding is consistent with, but not necessary to confirm, damage to afferent projections to the FOR, as determined by the model. Malfunction of Purkinje cells in the dorsal vermis, which inhibit the deep cerebellar nuclei, may cause opsoclonus by disinhibiting the FOR.

Acknowledgements

Supported by Canadian Institutes of Health Research Grants MT 15362 and ME 5404 (JAS), the Vision Science Research Program (University of Toronto) (AMW), and the E.A. Baker Foundation, Canadian National Institute for the Blind (AMW).

Appendix A

Simulations on the model shown in Fig. 10 were performed in Simulink (Mathworks). All simulations used a second order plant described by [46]:

$$H_p = \frac{1}{(0.15s+1)(0.004s+1)} \quad (1.1)$$

where s is the laplace transform. The bust neurons were also as in Van Gisbergen and have an activation function described by:

$$\text{Burst} = b_{\text{m}}(1 - \text{e}^{(\text{e}_{\text{m}}+\text{e}_{\text{o}})/b_{\text{k}}}) \quad (1.2)$$

where b_{m} is the maximum firing rate set at 1100 Hz, b_{k} is a constant, e_{m} is the input and e_{o} is the saturation, set here for 2° (see Van Gisbergen et al. [46] for a full description of the bust neurons). Gain1 in the feedback pathway was reduced to 0.72 in order to simulate hypermetric saccades, which were later corrected by the addition of the FOR. The high pass filter seen in the lower pathway was designed so that its output is an approximation of eye velocity. It is described by:

$$H_{\text{v}} = \frac{s}{0.009s + 1} \quad (1.3)$$

The contralateral FOR was simulated by adding a signal 8 ms before the onset of all saccades. This signal was simply obtained by calculating the appropriate eye velocity necessary to achieve a saccade of given amplitude and feeding it into the comparator, labeled 'C' in the figure. This signal represented the eye velocity portion of the saccadic plan. The delay of the feedback pathway (ipsilateral FOR) was adjusted to represent the necessary deceleration needed to drive the system. In order to induce oscillations, the gain (Gf) was increased to an appropriate amount as indicated in the text.

References

[1] Digre KB. Opsoclonus in adults. Report of three cases and review of the literature. Arch Neurol 1986;43:1165–75.
[2] Dichgans J, Jung R. Opsoclonus. Elmsford, New York: Pergamon; 1975.
[3] Hoyt WF, Daroff RB. Supranuclear disorders of ocular control systems in man. In: Bach-y-Rita P, Collins CC, Hyde JE, editors. The Control of Eye Movements. Orlando, FL: Academic Press 1971:191–3.
[4] Jung R, Kornhuber HH. Results of electronystagmography in man. In: Bender MB, editor. The oculomotor system. New York: Paul Hoeber; 1964. p. 442.
[5] Sharpe JA, Fletcher WA. Saccadic intrusions and oscillations. Can J Neurol Sci 1984;11:426–33.
[6] Leigh RJ, Zee DS. The neurology of eye movements. 3rd edn. Philadelphia: Oxford Univ. Press; 1999.
[7] Gresty MA, Findley LJ, Wade P. Mechanism of rotatory eye movements in opsoclonus. Br J Ophthalmol 1980;64:923–5.
[8] Zee DS, Robinson DA. A hypothetical explanation of saccadic oscillations. Ann Neurol 1979;5:405–14.
[9] Hormigo A, Dalmau J, Rosenblum MK, River ME, Posner JB. Immunological and pathological study of anti-Ri-associated encephalopathy. Ann Neurol 1994;36:896–902.
[10] Cogan DG. Opsoclonus, body tremulousness, and benign encephalitis. Arch Ophthalmol 1968;79:545–51.
[11] Ellenberger CJ, Campa JF, Netsky MG. Opsoclonus and parenchymatous degeneration of the cerebellum. Neurology 1968;18:1041–6.
[12] Alessi D. Lesioni parenchimatose del cervelleto da carcinoma uterino (gliosi carcinotossica?). Riv Patol Nerv Ment 1940;55:148–74.
[13] Ross AT, Zeman W. Opsoclonus, occult carcinoma, and chemical pathology in dentate nuclei. Arch Neurol 1967;17:546–51.
[14] Dalmau JO, Posner JB. Paraneoplastic syndromes. Arch Neurol 1999;56:405–8.
[15] Sutton I, Winer J, Rowlands D, Dalmau J. Limbic encephalitis and antibodies to Ma2: a paraneoplastic presentation of breast cancer. J Neurol, Neurosurg Psychiatry 2000;69:266–8.
[16] Sharpe JA, Goldberg HJ, Lo AW, Herishanu YO. Visual–vestibular interaction in multiple sclerosis. Neurology 1981;31:427–33.
[17] Huaman AG, Sharpe JA. Vertical saccades in senescence. Invest Ophthalmol Visual Sci 1993;34:2588–95.
[18] Balliet R, Nakayama K. Training of voluntary torsion. Invest Ophthalmol Visual Sci 1978;17:303–14.
[19] Ranalli PJ, Sharpe JA. Vertical vestibulo-ocular reflex, smooth pursuit and eye-tracking dysfunction in internuclear ophthalmoplegia. Brain 1988;111:1299–317.
[20] Vignaendra V. Electro-oculographic analysis of opsoclonus: its relationship to saccadic and non-saccadic eye movements. Neurology 1977;27:1129–33.
[21] Ellenberger CJ, Keltner JL, Stroud MH. Ocular dyskinesia in cerebellar diseases: evidence for the similarity of opsoclonus, ocular dysmetria and flutter-like oscillations. Brain 1972;95:685–92.
[22] Brumlik J, Means ED. Tremorine—tremor, shivering and acute cerebellar ataxia in the adult and child—a comparative study. Brain 1969;92:157–90.
[23] Morrow MJ, Sharpe JA. Torsional nystagmus in the lateral medullary syndrome. Ann Neurol 1988;24:390–8.
[24] Lopez L, Bronstein AM, Gresty MA, Rudge P, DuBoulay EP. Torsional nystagmus. A neuro-otological and MRI study of thirty-five cases. Brain 1992;115:1107–24.
[25] Weissman JD, Seidman SH, Dell'Osso LF, Naheedy MH, Leigh RJ. Torsional, see-saw, "bow-tie" nystagmus in association with brainstem anomalies. Neuro-Ophthalmology 1990;10:315–8.
[26] Dehaene I, Casselman JW, Van Zandijcke M. Unilateral internuclear ophthalmoplegia and ipsiversive torsional nystagmus. J Neurol 1996;243:461–4.
[27] Rosenthal JG, Selhorst JB. Continuous non-rhythmic cycloversion. Neuro-Ophthalmology 1987;7:291–5.
[28] Luque FA, Furneaux HM, Ferziger RAB, Rosenblum MK, Wray SH, Schold SCJ, et al. Anti-Ri: an antibody associated with paraneoplastic opsoclonus and breast cancer. Ann Neurol 1991;29:241–51.
[29] Hersh B, Dalmau J, Dangond F, Gultekin S, Geller E, Wen PY. Paraneoplastic opsoclonus–myoclonus associated with anti-Hu antibody. Neurology 1994;44:1754–5.
[30] Noetzel MJ, Cawley LP, James VL, Minard BJ, Agrawal HC. Anti-neurofilaments protein antibodies in opsoclonus–myoclonus. J Neuroimmunol 1987;15:137–45.
[31] Kaneko CRS. Effects of ibotenic acid lesions of the omnipause neurons on saccadic eye movements in Rhesus Macaques. J Neurophysiol 1996;75:2229–42.
[32] Ridley A, Kennard C, Scholtz CL, Buttner-Ennever JA, Summers B, Turnbull A. Omnipause neurons in two cases of opsoclonus associated with oat cell carcinoma of the lung. Brain 1987;110:1699–709.
[33] Optican LM, Robinson DA. Cerebellar-dependent adaptive control of primate saccadic system. J Neurophysiol 1980;44:1058–76.
[34] Westheimer G, Blair SM. Functional organization of primate oculomotor system revealed by cerebellectomy. Exp Brain Res 1974;21:463–72.
[35] Robinson FR, Straube A, Fuchs AF. Role of the caudal fastigial nucleus in saccadic generation: II. Effects of muscimol inactivation. J Neurophysiol 1993;70:1741–58.
[36] Ohtsuka K, Sato H, Noda H. Saccadic burst neurons in the fastigial nucleus are not involved in compensating for orbital nonlinearities. J Neurophysiol 1994;71:1976–80.
[37] Lefevre P, Quaia C, Optican LM. Distributed model of control of saccades by superior colliculus and cerebellum. Neural Networks 1998;11:1175–90.

[38] Quaia C, Lefevre P, Optican LM. Model of the control of saccades by superior colliculus and cerebellum. J Neurophysiol 1999;82: 999–1018.
[39] Noda H, Sugita S, Ikeda Y. Afferent and efferent connections of the oculomotor region of the fastigial nucleus in the macaque monkey. J Comp Neurol 1990;302:330–48.
[40] May PJ, Hartwich-Young R, Nelson J, Sparks DL, Porter JD. Cerebellotectal pathways in the macaque: implications for collicular generation of saccades. Neuroscience 1990;36:305–24.
[41] Fuchs AF, Robinson FR, Straube A. Role of the caudal fastigial nucleus in saccade generation: I. Neuronal discharge pattern. J Neurophysiol 1993;70:1723–40.
[42] Helmchen C, Straube A, Buttner U. Saccade-related activity in the fastigial oculomotor region of the macaque monkey during spontaneous eye movements in light and darkness. Exp Brain Res 1994; 98:474–82.
[43] Ohtsuka K, Noda H. Direction selective saccadic burst neurons in the fastigial oculomotor region of the macaque. Exp Brain Res 1990;81:659–62.
[44] Ohtsuka K, Noda H. Saccadic burst neurons in the oculomotor region of the fastigial nucleus of the macaque monkey. J Neurophysiol 1991;65:1422–34.
[45] Robinson D. Oculomotor control signals. In: Lennerstrand G, Bach-y-Rita Y, editors. Basic mechanism of ocular motility and their clinical implications. Oxford: Pergamon; 1975. p. 337–74.
[46] Van Gisbergen JA, Robinson DA, Gielen S. A quantitative analysis of generation of saccadic eye movements by burst neurons. J Neurophysiol 1981;45:417–42.
[47] Scudder CA. A new local feedback model of the saccadic burst generator. J Neurophysiol 1988;59:1455–75.
[48] Van Gisbergen J, Van Opstal A. Models. In: Wurtz RH, Goldberg ME, editors. The neurobiology of saccadic eye movements. North Holland: Elsevier; 1989. p.69–101.
[49] Dean P. Modelling the role of the cerebellar fastigial nuclei in producing accurate saccades: the importance of burst timing. Neuroscience 1995;68:1059–77.
[50] Tweed DB, Vilis T. The superior colliculus and spatiotemporal translation in the saccadic system. Neural Networks 1990;3:75–86.
[51] Grossberg S, Kuperstein M. Neural dynamics of adaptive sensory–motor control. New York: Pergamon; 1989.
[52] Arai K, Keller EL, Edelman JA. Two-dimensional neural network model of the primate saccadic system. Neural Networks 1994;7: 1115–35.
[53] Van Opstal AJ, Kappen H. A two-dimensional ensemble coding model for spatial–temporal transformation of saccades in monkey superior colliculus. Network 1993;4:19–38.
[54] Waitzman DM, Ma TP, Optican LM, Wurtz RH. Superior colliculus neurons mediate the dynamic characteristics of saccades. J Neurophysiol 1991;66:1716–37.